

Burg power spectral density-based characterization of Doppler blood flow sound during hemorrhoidal artery ligation

Daniel Santoso^{1,2}, Oyas Wahyunggoro¹, Prpto Nugroho¹

¹Department of Electrical and Information Engineering, Universitas Gadjah Mada, Yogyakarta, Indonesia

²Department of Electronics and Computer Engineering, Universitas Kristen Satya Wacana, Salatiga, Indonesia

Article Info

Article history:

Received Oct 29, 2021

Revised Apr 15, 2022

Accepted May 16, 2022

Keywords:

Characterization

Doppler sound

Hemorrhoidal artery ligation

K-means clustering

Power spectral density

ABSTRACT

Hemorrhoidal artery ligation (HAL) has become universally accepted minimally invasive treatment of hemorrhoids disease. HAL involves precise identification of the superior rectal arteries supplying hemorrhoidal tissues using ultrasonic Doppler principles. During this process, at least there are three distinct sounds may be encountered by the surgeon. Only the pulsing Doppler sound is useful as it indicates the presence of hemorrhoidal artery. The accuracy based on traditional auscultation is commonly affected by surgeon's hearing sensitivity and clinical experience. Therefore, automatic Doppler blood flow sound will be a great help in locating hemorrhoidal arteries. In this paper, a method based on the center frequency and kurtosis features extracted from Burg's power spectral density (PSD) to distinguish three different types of Doppler blood flow sound signal during HAL procedure is proposed. Separability measurement was carried out using K-means clustering with the city block distance and three clusters corresponding to different sound types are successfully formed. In terms of arterial sound detection, an accuracy of 94.11% can be achieved. This result suggests that centre frequency, kurtosis, and maybe some other statistical features extracted from Burg PSD have the potential to be utilized as a means in automatic Doppler blood flow sound recognition.

This is an open access article under the [CC BY-SA](https://creativecommons.org/licenses/by-sa/4.0/) license.



Corresponding Author:

Daniel Santoso

Department of Electrical and Information Engineering, Universitas Gadjah Mada

2nd Grafika Road, Yogyakarta, Special Region of Yogyakarta, Indonesia

Email: daniel.santoso@mail.ugm.ac.id

1. INTRODUCTION

The surgical intervention techniques of hemorrhoids disease have advanced over past the three decades. Traditional surgical hemorrhoidal excision is notorious for significant postoperative pain and impaired anal function due to the deformation of anal canal anatomy. These problems have encouraged surgeons to adopt minimally invasive procedures in treating hemorrhoids disease. Since its invention in 1995 by Morinaga *et al.* [1], hemorrhoidal artery ligation (HAL) has become a widely accepted procedure for handling hemorrhoids disease. In comparison with excisional methods, HAL excels at the absence of anal lacerations, which in turn reduces patient's postoperative pain and uncomfortable feelings. Anal anatomy and physiology preservation cannot be underrated as well [2]. Several studies suggest that early and midterm outcomes have shown great recovery and positive patient feedbacks [3]. Dearterialization technique, in comparison with other non-excisional procedures, such as stapled hemorrhoidopexy may have additional benefit of minimizing life-threatening complications [4].

The reasoning for HAL procedure is based on the presumption that blood flowing through rectal artery to hemorrhoidal tissues cannot recirculate given the absence of capillary intercession between the

arterial and venous systems inside the anal canal. This blood overflow eventually causes the dilatation of hemorrhoidal tissues. HAL involves the precise marking of of rectal artery branches supplying hemorrhoidal tissues using an ultrasonic transducer linked to the outer surface of a proctoscope. Identified hemorrhoidal arteries, which are commonly surrounding the anus in the odd-numbered clock positions [5], are then suture ligated through a ligation window within the proctoscope. Ligation of these arteries significantly reduces blood passage into the hemorrhoidal venous plexi and later causes the hemorrhoidal tissues shrink gradually.

Hemorrhoidal arteries identification in HAL procedure is based on the Doppler ultrasound principles. To properly detect each hemorrhoidal artery within the rectal column, the surgeon conducting the HAL surgery relies solely on the Doppler sound emitted by the Doppler processor. There are two major constrains of Doppler sound auscultation. The first one is related to the interpretation of the audible output by the surgeon, as pointed out by Mowatt *et al* [6]. The inaccurate interpretation of Doppler ultrasound outputs may arise from inadequate training, lack of experience, and time constraints [7]–[9]. The second one is that the surgeon must listen very carefully to detect subtle changes in Doppler ultrasound outputs [10].

Generally speaking, the accuracy based on traditional auscultation is highly affected by observer's hearing sensitivity and clinical experience [11]. Therefore, a computerized assisting tool to analyze Doppler ultrasound signal can be beneficial to recognize certain Doppler sound that indicates haemorrhoidal arterial blood flow. However, Doppler sound signal produced by ultrasound machine is rarely recorded and investigated, including the one associated with hemorrhoidal artery [12]. Thus far, most research has focused on other biological sounds such as heart sound (HS) and lung sound (LS). Therefore adopting methods from studies regarding HS and LS analysis is very relevant to keep methods that will be used right on the cutting edge. Doppler blood flow sound, HS, and LS share common audible frequency spectrum and they all represent a non-stationary signal [10], [13]–[17].

Despite the limited number of studies addressing Doppler sound signal analysis, some literatures are accessible that could serve as a steppingstone. One of the preliminary works in investigating Doppler sound signal characteristics was conducted by Guler and Kara [18] who used fast fourier transform (FFT) and autoregressive (AR) modelling methods to perform spectral analysis of Doppler sound signal produced by healthy and stenosis mitral valve. It was reported that spectrogram of healthy subject had two peaks and a valley between them while for the subject suffering mitral stenosis, the valley was absent. Later, Guler *et al.* Proposed an automated diagnosis method to distinguish Doppler sound signals acquired from both healthy subjects and subjects having ophthalmic arterial (OA) and internal carotid arterial (ICA) diseases [19]. The method involved statistical features: maximum, mean, minimum, and standard deviation calculated from time – frequency representations of Doppler blood flow sound signals. The extracted features of different categories of OA and ICA signals were different from each other so they can serve as discriminating parameters in classifying Doppler signals. In this study, the authors also mentioned that performing spectral analysis is the most complete way to present blood flow information contained in the Doppler shift signal. Maximum envelope of the carotid artery Doppler spectrogram derived from AR method was used by Ozsen for diagnosing atherosclerosis disease [20]. It was found that subjects with atherosclerosis have lower maximum frequency envelope values. According to Tedim *et al.* [21] was the first to search automatic methods to improve venous air embolism (VAE) detection using precordial Doppler placed on human patients during real surgeries. VAE may occur during surgical procedures and may lead to serious complications such as stroke or cardiovascular failure. VAE event, which is indicated by turbulent blood flow, was simulated by using saline administrations through peripheral and central catheters. Frequency component of Doppler sound signal was examined by power spectral density (PSD) estimation by using Welch method. Different kinds of spectral features including frequency correlating with maximum power of PSD, 95% power of PSD, and half power of PSD were then extracted to characterize the power distribution attribute. Observations showed that frequency corresponding to 95% power of PSD was the most sensitive to detect blood flow turbulence whereas frequency corresponding to half power of PSD remained unchanged.

As for HS and LS, more research had been conducted to study their characteristics [22]. A research performed by Theo *et al.* [23]. Assessed the feasibility of using the analysis of power spectral to compute the ratio between the sum of the powers in the N highest peaks in the power spectral to that of the entire power spectral for each fundamental HS state. This feature can be used to classify normal or abnormal HS. Kristomo *et al.* [24] presented a method based on the statistics calculation from autoregressive–power spectral density (AR–PSD) extracted from HS. These statistics were used as inputs for the classification of abnormal HS into 9 types. Research by Schmidt *et al.* [25] weak murmurs in HS were used to detect coronary artery disease (CAD) by dividing HS into five different frequency bands and nine features were extracted from those bands. A multivariate classifier based on quadratic discriminant analysis (QDA) was used to construct CAD score from the features. According to Akanksha *et al.* [26] with a similar goal collected HS from four locations on chest and was analysed using cross power spectral density (CPSD). Four separate features, including relative power, power ratio to adjacent subbands, mean and standard deviation were computed from CPSD. Support vector machine (SVM) was then used as a classifier. Different power spectral characteristics estimated from

LS may also be used to indicate pulmonary chronic lung diseases, as investigated in [27], [28]. K-means algorithm, one of the most widely used clustering approaches, was also used to separate Mel-frequency spectral coefficient (MFCC) features within first and second HS segments (S1 and S2, respectively) into two groups [29]. A population center vector for each group was then calculated to form a supervector, which was used as input for a deep neural network (DNN) classifier. The results revealed improvement in terms of accuracy by employing k-means prior to the classification process. Jamal *et al.* [30] added murmur components in HS analysis in addition to S1 and S2 detection by using time-frequency method. Research by Hadiyoso *et al.* [31] took advanced approach by implementing an electronic stethoscope that enabled the findings on auscultation to be sent to a cloud server for more advanced analysis. Android-based mobile phone and Steder application were used as a communication device and sound data manager, respectively. The prototype of the system was successfully developed and usable but had not been tested yet in real situations.

From the literature review, it is discovered that power spectral analysis has promising opportunity in characterizing Doppler sounds. In this paper, a simple method to distinguish different types of Doppler blood flow sound signal during HAL procedure is proposed. Burg's PSD is applied to estimate the band power of different blood flow sound signals which is grouped into three classes. Statistical features extracted from the signal power bands are expected to provide means to accurately distinguish the sound signals into predetermined classes. Performance evaluation is based on t-test and k-means clustering with city block distance.

2. MATERIALS AND METHODS

2.1. Processing steps

The standard procedure for computerized PCG processing and analysis can be outlined into the following sequences: i) pre-processing; ii) feature extraction; iii) classifier modeling [16]. The characterization problem in this study was also resolved according to the procedure with several required adjustments.

Doppler sounds were acquired using an 8 MHz transducer that gently moved around the wrist area to scan for any blood movement inside radial artery. Rather than a real site inside the anal canal, the wrist area was selected because of the ease of access and similar Doppler produced. This approach was approved by collaborating surgeon. The processor received the frequency-shifted signal from the transducer and generated a Doppler signal with a frequency within the audible band. A Bluetooth-enabled portable amplifier was used to amplify the signal. The Doppler audible sounds were captured by using a digital sound recorder with a 44.1 kHz sampling rate.

The first processing step was to reduce the sound sample to a single arterial pulse cycle, with approximately 0.7 s duration. Then the sample was resampled at a sampling frequency of 8820 Hz and followed with amplitude normalization. Next, the power spectral of the sample was analyzed using Burg method while transforming the sample into a frequency domain. After that, features were extracted from PSD curve and analyzed for the most suitable features for classification. Finally, separability measurement was performed to determine whether selected features can be used to discriminate one type of sound from another. A total of 51 sound samples used, separated into classes: arterial, venous, and probe rubbing sounds. Figure 1 shows the system flowchart for the characterization of Doppler blood flow sound during HAL.



Figure 1. Flowchart of characterization process

2.2. Doppler blood flow detection principle

The Doppler effect refers to the frequency shift of a signal reflected from a moving object to its observer perception. Doppler signal can be possibly obtained from blood flow since blood contains red blood cells as scattering particles. If the blood flow is toward the transducer, the perceived frequency will be higher and vice versa. Figure 2 illustrates an ultrasound beam being transmitted from the transducer toward red blood cells at a certain angle of attack θ . The beam hits the objects and returns with a Doppler-shifted frequency to the receiver. The Doppler shift fd of an ultrasound signal with the nominal frequency fc is given by (1):

$$f_D = \left(\frac{2v \cos \theta}{c} \right) f_c \tag{1}$$

Where v is the velocity of the scattering objects and c is the propagation speed of sound waves in the medium. The scattering object in this case is red blood cells flowing inside haemorrhoidal vessels with a normal velocity of 20 to 750 mm/s [32]. Sound waves travel in soft tissue at an average speed of 1540 m/s [33]. The frequency f_c for blood flow detection application is in the range of 2 to 10 MHz, resulting in a Doppler shift in the audible range of 0.2 to 7.5 kHz.

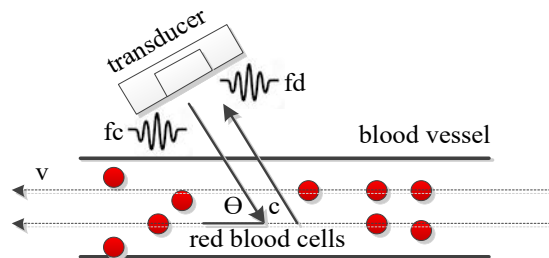


Figure 2. Doppler-shifted frequency f_d appears as an audible sound as the reflected beam received by the transducer

Doppler sound waveforms are commonly defined as triphasic. The key components of a Doppler sound waveform include: (i) primary forward flow due to contraction of left ventricle during systole; (ii) transient reversal flow as a result of backscattering from outflow bed with a high resistance in early diastole; (iii) secondary forward flow due to reflection from a closed aortic valve during late systole [34]. In Figure 3, both Doppler sound and PCG waveform are plotted together to show the relationship between them in time domain.

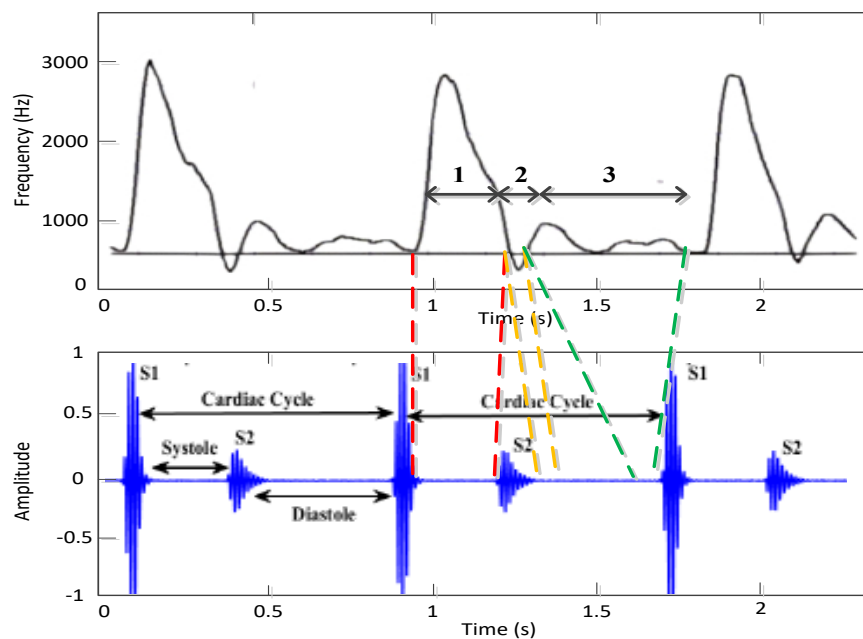


Figure 3. Doppler sound waveform and four states of cardiac cycle (S1, systole, S2, diastole) presented [34], [35]

Different Doppler signals are produced depending on the position of the artery, distance from the transducer, and direction of blood flow in relation to the ultrasound waves emitted by the transducer. In terms of intensity, the more perpendicular the blood flow to the ultrasound waves the higher the Doppler signal. Conversely, the more parallel the blood flow is, the lower the signal. The hemorrhoidal arteries are sought by slowly rotating and tilting the proctoscope inside the anal canal. During this process, at least three different sounds may be encountered by the surgeon, namely; pulsing, wheezing, and thumping sounds. Pulsing sound reflects pulsatile blood movement inside an artery, wheezing sound reflects non-pulsatile venous velocity,

and thumping sound results from rubbing action between transducer and rectum wall. Only the pulsing Doppler sound indicates the presence of hemorrhoidal artery, characterized by middle–low frequency spectrum (up to 4 kHz) with pulsing amplitude. The return echoes from steady blood stream may occur when venous blood vessels pass through the region of Doppler sensitivity [36].

2.3. PSD estimation

PSD describes how the power of a signal is distributed along frequency. The Wiener–Khinchine theory suggests that the PSD of a wide–sense stationary random process $x(t)$ is the Fourier transformation of the autocorrelation of the signal [37]. This definition can be derived using (2) to (4):

$$F[x(t)] = X(\omega) = \int_{-\infty}^{\infty} x(t)e^{-j\omega t} dt \quad (2)$$

$$R(\tau) = x(\tau) * x(-\tau) = \int_{-\infty}^{\infty} x(t)x(t + \tau) dt \quad (3)$$

$$F[R(\tau)] = \int_{-\infty}^{\infty} R(\tau)e^{-j\omega t} d\tau \quad (4)$$

Autoregressive (AR) based model is one of the parametric methods used to estimate the PSD of a signal. AR models use a linear predictive method to extrapolate the signal beyond its existing values and predict the output of a system based on previous outputs [37]. Such parametric method provides a fine frequency resolution but is sensitive to order selection. A model with an extremely low order produces an over–smoothed spectral whereas an extremely order tends to produce false low–level peaks in the spectral. An AR model can be defined as in (5):

$$x(t) = \sum_{i=1}^p a_i x_{t-i} + \varepsilon(t) \quad (5)$$

Where a_i are the AR coefficients, p is the order of model, and $\varepsilon(t)$ represents noise. The PSD estimation by using an AR model is expressed by (6):

$$\hat{P}_{AR}(f) = \frac{\varepsilon_p}{|1 + \sum_{k=1}^p a_p(k)e^{-2\pi jkf}|^2} \quad (6)$$

Burg is one of the several methods available to estimate AR coefficients. In Burg method, AR parameters are found by minimizing (least squares) errors of sums of forward and backward linear prediction. Such minimization occurs with the AR coefficients constrained to satisfy the Levinson–Durbin recursion algorithm.

2.4. Statistical features

Abundant statistical features are available to be extracted from data both in time and frequency domains. Some of the features that are relevant to this study are listed below.

- a. Mean: the arithmetic mean μ is the average of values $\{x_1, x_2, \dots, x_m\}$ located within a certain data range. It is expressed by (7):

$$\mu = \frac{1}{m} \sum_{i=1}^m x_i \quad (7)$$

- b. Standard deviation: standard deviation can be calculated using (8). It is an indication how values $\{x_1, x_2, \dots, x_m\}$ are spread out.

$$\sigma = \sqrt{\frac{1}{m} \sum_{i=1}^m (x_i - \mu)^2} \quad (8)$$

- c. Skewness: skewness is one of the features that is used to measure the shape of the data set, particularly the asymmetry. It is expressed as in (9):

$$Sk = \frac{\mu_3}{\sigma^4} \quad (9)$$

Where μ_3 is the 3rd moment about the mean.

- d. Kurtosis: similar to skewness, kurtosis provides information about the shape of the data set. It is a measure of the “tailedness” of the probability distribution of the data. The formula is given by (10):

$$Ku = \frac{\mu_4}{\sigma^4} \quad (10)$$

- e. Entropy: the entropy of a random variable is used to determine how unpredictable it is. The entropy H of a discrete variable X with possible values $\{x_1, x_2, \dots, x_m\}$ and probability mass function $p(X)$ is given by (11):

$$H(X) = -\sum_{i=1}^m P(x_i) \cdot \log_2 P(x_i) \quad (11)$$

- f. Frequency related: Figure 4 shows the typical PSD estimation result in the frequency domain and graphical parameters that can be extracted from it.

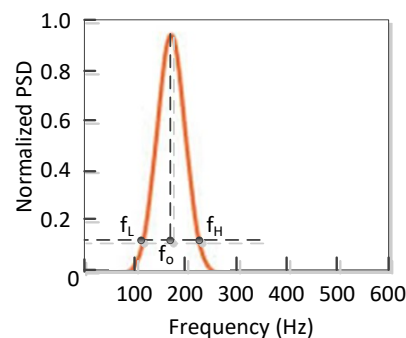


Figure 4. Typical PSD estimation curve with available features

2.5. K-means clustering

Clustering is one of the most popular analytic data identification methods used to provide a view of the the data structure. This process identifies homogenous subgroups within the data such that data points in each group are as similar as possible in accordance with several similarity measures. Clustering is categorized as unsupervised learning given that no ground truth exists for evaluation of the clustering performance.

K-means clustering is considered as one of the most usable clustering algorithms since it is simple and fast. This procedure iteratively attempts to partition a certain dataset into k pre-defined individual non-overlapping clusters, in which each datum belongs only to one cluster. It works through the following steps [38]:

- Choose k starting centers arbitrarily $C = \{c_1, \dots, c_k\}$.
- Set cluster C_i to be the set of points in X that are closer to c_i than they are to c_j for all $j \neq i$, for each $i \in \{1, \dots, k\}$.
- Set c_i to be the center of mass of all points in C : $c_i = \frac{1}{|C_i|} \sum_{x \in C_i} x$, for each $i \in \{1, \dots, k\}$.
- Repeat steps 2 and 3 until C remains constant.

For the k-means problem, given an integer k and a set of n data points $X \subset \mathbb{R}^d$. It is required to choose k centers C so as to minimize the potential function in (12) [39]:

$$\varphi = \sum_{x \in C} \min_{c \in C} \|x - c\|^2 \quad (12)$$

In k-means clustering, data points are assigned to the centroid with a minimum distance based on the values found. Therefore, distance calculation plays an important role in this clustering algorithm. Several different techniques are available to compute distance between two points such as city block, Euclidean, cosine, and correlation distances. For city block distance between two points a and b with k dimensions is defined as in (13) [39]:

$$d(a, b) = \sum_{j=1}^k |a_j - b_j| \quad (13)$$

Separability evaluation was performed to observe whether statistical features extracted from PSD can be used to differentiate one type of sound from another. K-means clustering with a city block distance was used for the testing purpose. Clustering performance can be evaluated using a measure such as accuracy which is defined as in (14):

$$accuracy = \frac{true_{pos} + true_{neg}}{true_{pos} + true_{neg} + false_{pos} + false_{neg}} \times 100\% \quad (14)$$

3. RESULTS AND DISCUSSION

Three kinds of sounds are normally perceived by the surgeon from the Doppler processor through the HAL procedure. However, only the pulsing blood flow sound is useful for the surgeon as a location marker of hemorrhoidal arteries. The wheezing sound is produced when the ultrasound wave hits blood particles flowing in the vein. When proctoscope is being rotated inside the anal canal in attempt to search hemorrhoidal arteries, random rubbing sound is also produced by Doppler processor. The latter two mentioned sounds are not sounds of interest for the surgeon. Figure 5 shows the three kinds of Doppler sounds that commonly encountered during HAL procedure in the time domain.

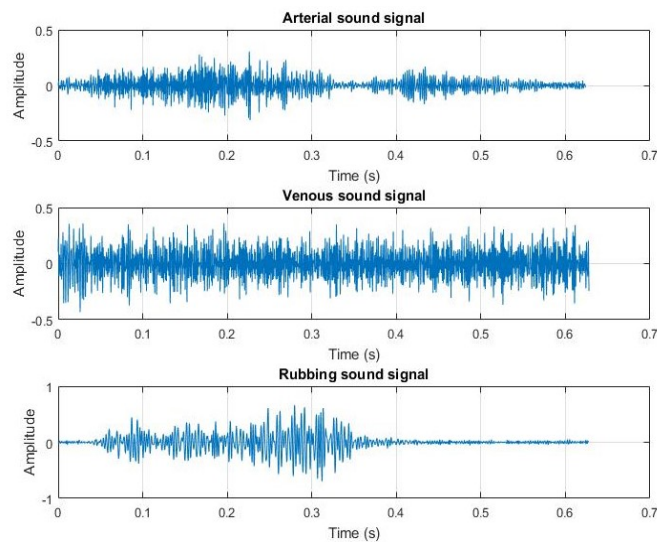


Figure 5. Sound fragments representing the three classes of Doppler blood flow sound

Using Burg's PSD the Doppler sounds were transformed into the frequency domain after normalization and downsampling. The purpose of this transformation is to obtain the features of each Doppler sound mentioned previously. The transformation results are illustrated in Figure 6. Figures 6(a), (b), and (c) are the results of arterial, venous, and rubbing sound sample respectively. A brief observation of the figure reveals that all three Doppler sounds have significant frequency components up to 2000 Hz. However, different sounds exhibit varied peak characteristics. The PSD estimation for arterial sound has high-low peaks while venous sound counterpart has two nearly identical peaks. In the other hand, rubbing sound PSD estimation only consists of a single peak with narrower bandwidth. In this study, only features related to shape of data set were extracted from PSD estimation that is center frequency, kurtosis, entropy, and skewness. Table 1 shows the PSD estimation features extraction result.

Table 1. Extracted features from PSD estimation of all Doppler blood flow sounds

Doppler sound	Center frequency (Hz)	Kurtosis	Entropy	Skewness
Arterial	434.71 ± 17.79	26.37 ± 7.07	2.98 ± 0.15	4.48 ± 0.70
Venous	486.39 ± 31.37	13.07 ± 4.17	2.58 ± 0.57	3.13 ± 0.58
Rubbing	314.13 ± 14.32	55.35 ± 8.31	1.38 ± 0.14	6.91 ± 0.55

From this data, it can be observed that the center frequencies of all sounds are relatively uniformed, indicated by a slight standard deviation. For kurtosis feature, despite the wide deviation, no overlap is observed between sounds. The entropies of all sounds converge into small values with a relatively large standard deviation causing the entropies of arterial and venous sounds to overlap. Skewness shows slightly higher average values and lower standard deviation compared to entropy but without the overlap. Furthermore, t-test was performed to statistically demonstrate class separation, as described in [40].

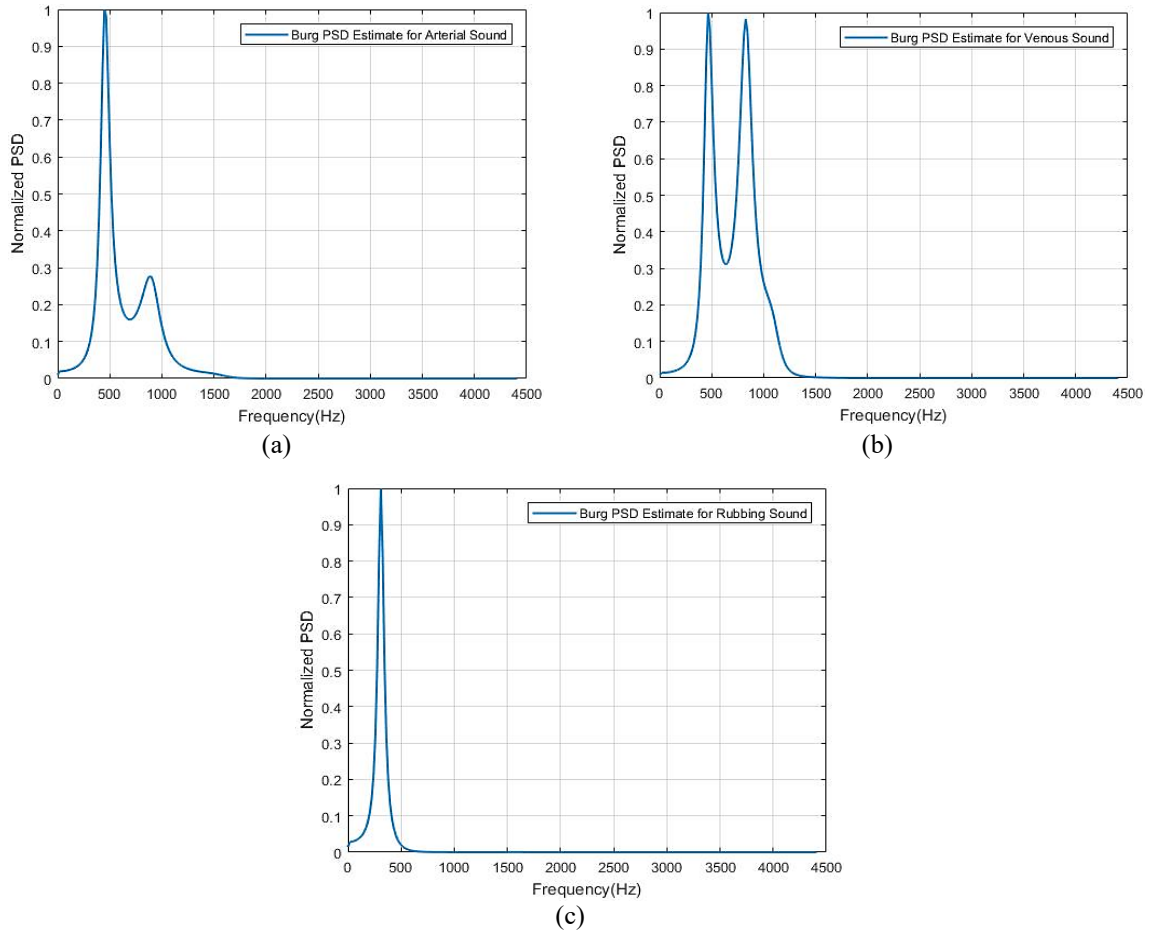


Figure 6. PSD estimation of (a) arterial, (b) venous, and (c) rubbing sound sample

Figure 7 illustrates that normalized value statistical features is separable. This result is confirmed by t-test tabulated in Table 2. The t-test is an inferential statistic calculated from the value of center frequency, kurtosis, entropy, and skewness features to determine whether there is significant difference between the means of two groups, arterial or non-arterial (venous and rubbing) sounds in this case. The range of p-value was found by calculating t-score with the significance level of 0.05. Table 2 proves that all of the p-values fall in the significance range, therefore demonstrating that values of features are separated.

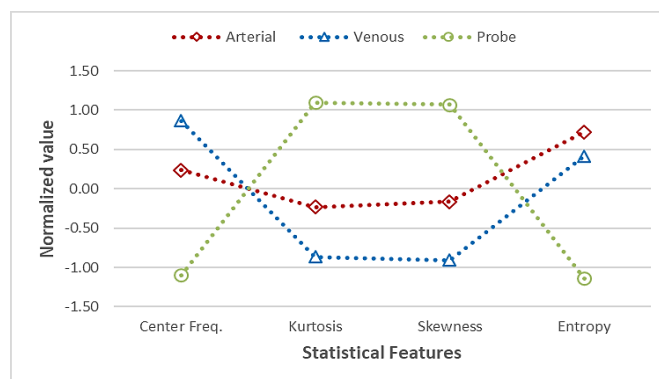


Figure 7. Normalized value of statistical features

In this study, center frequency and kurtosis were chosen as key features to distinguish arterial, venous, and rubbing sounds because of their particular characteristics. Center frequency is relatively uniform while kurtosis is quite spaced away between one sound type to another. The center frequency and kurtosis as

discerning features were tested using k-means clustering with the city block distance. At the end of iterative process, the data should be distributed into the three different clusters corresponding to three Doppler sounds discussed previously. The result of k-means clustering is illustrated as scatter diagram in Figure 8.

It can be readily seen that the plotting of two features center frequency and kurtosis shows three different areas along with their own center points. The system is expected to correctly detect arterial sound, therefore accuracy for this detection needs to be investigated. Based on the clustering, the numbers of true positive, true negative, false positive, and false negative samples are 15, 33, 2, and 1 sample respectively. This yields accuracy of 94.11% for arterial sound detection by using (14). These findings confirm our hypothesis that arterial, venous, and rubbing sounds may be recognized by extracting statistical features from PSD estimation of the sound signal. In addition, the fact that power spectral analysis is shown to be effective in Doppler blood flow sound characterization is consistent with the discoveries which mainly reported in [18]-[21], [23]-[29].

Table 2. T-score and p-value calculated from four statistical features

Feature	t-score	p-value
Center frequency	10.4981	0.0129
Kurtosis	-9.5670	0.0104
Entropy	35.6868	<0.0001
Skewness	-6.6680	0.0416

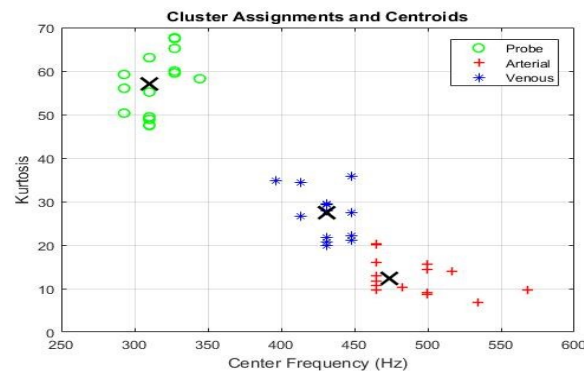


Figure 8. Scatter diagram of center frequency and kurtosis

4. CONCLUSION

In this work, an effort has been conducted to characterize and classify three different Doppler sounds that usually encountered during HAL procedure. The work involved the Burg method to estimate PSD of the sound signal and the estimation curves suggested that each sound type has its own specific shape. Statistical features were extracted from the PSD estimation and it was discovered by using t-test that center frequency, kurtosis, entropy, and skewness normalized value is separable. Therefore, those features are suitable to describe PSD estimation curve quantitatively. Separability measurement was further carried out using k-means clustering with center frequency and kurtosis as selected features and three clusters corresponding to the three different sound types were successfully formed. In terms of arterial sound detection, an accuracy of 94.11% can be achieved without further signal processing. These results suggest that center frequency, kurtosis, and maybe some other statistical features extracted from Burg PSD have the potential to be utilized as a means in automatic Doppler blood flow sound recognition. In the near future with the collection of more data, the effectiveness of the proposed method should be investigated. The ultimate goal is real-time hardware implementation of the mentioned system that can be used as an automatic tool in clinical setup.

ACKNOWLEDGEMENTS

This study was completed because of good cooperation of the authors. We would like to thank Direktorat Riset dan Pengabdian Masyarakat Kementerian Riset dan Teknologi-Badan Riset dan Inovasi Nasional (DRPM Kemenristek-BRIN), contract number 6/E1/KP.PTNBH/2021 and Direktorat Penelitian Universitas Gadjah Mada (Dit. Lit. UGM), contract number 2308/UN1/DITLIT/DIT-LIT/PT/2021 for

supporting this research under Penelitian Disertasi Doktor (PDD) program. Special thanks are addressed to Dr. Risanuri Hidayat for knowledge sharing regarding feature extraction. We would also like to thank Dr. Sugandi Hardjanto, Sp. B., a surgeon from Kasih Ibu General Hospital, and his team for their assistance with data collecting.






REFERENCES

- [1] K. Morinaga, K. Hasuda, and T. Ikeda, "A novel therapy for internal haemorrhoids: ligation of the haemorrhoidal artery with a newly devised instrument (Moricorn) in conjunction with a Doppler flowmeter," *American Journal of Gastroenterology*, vol. 90, no. 4, pp. 610-613, 1995.
- [2] C. Ratto, A. Parello, and L. Donisi, F. Litta and G. B. Doglietto, "Anorectal physiology is not changed following transanal hemorrhoidal dearterialization for hemorrhoidal disease: clinical, manometric, and endosonographic features," *Colorectal Disease*, vol. 13, no. 8, pp. e243-e245, 2011, doi: 10.1111/j.1463-1318.2011.02665.x.
- [3] C. Ratto *et al.*, "Evaluation of transanal hemorrhoidal dearterialization as a minimally invasive therapeutic approach to hemorrhoids," *Diseases of the Colon and Rectum*, vol. 53, no. 5, pp. 803-811, 2010, doi: 10.1007/DCR.0b013e3181cdafa7.
- [4] A. Infantino, D. F. Altomare, C. Bottini, M. Bonanno and S. Mancini, "Prospective randomized multicentre study comparing stapler hemorrhoidopexy with Doppler-guided transanal hemorrhoid dearterialization for third-degree hemorrhoids," *Colorectal Disease*, vol. 14, no. 2, pp. 205-211, 2012, doi: 10.1111/j.1463-1318.2011.02628.x.
- [5] P. J. Gupta, S. Kalaskar, S. Taori and P. S. Heda, "Doppler-guided hemorrhoidal artery ligation does not offer any advantage over suture ligation of grade 3 symptomatic hemorrhoids," *Techniques in Coloproctology*, vol. 15, no. 4, pp. 439-444, 2011, doi: 10.1007/s10151-011-0780-7.
- [6] G. Mowatt *et al.*, "Systematic review of the clinical effectiveness and cost effectiveness of oesophageal Doppler monitoring in critically ill and high risk surgical patients," *Health Technology Assess*, vol. 13, no. 7, pp. 1-95, 2009, doi: 10.3310/hta13070.
- [7] J. Tweedie, "Pulse palpation and Doppler assessment in podiatric practice," *Podiatry Now*, vol. 3, pp.394-298, 2002.
- [8] S. A. Ray, P. D. Srodon, R.S. Taylor, and J. A. Dormandy, "Reliability of ankle: brachial pressure index measurements by junior doctors," *British Journal of Surgery*, vol. 81, no. 2, pp. 188-190, 1994, doi: 10.1002/bjs.1800810208.
- [9] V. Kaiser, A. M. Kester, H. E. Staffers, P. J. E. H. M. Kitslaar, and J. A. Knottnerus, "The influence of experience on the reproducibility of the ankle-brachial systolic pressure ratio in peripheral occlusive disease," *European Journal of Vascular and Endovascular Surgery*, vol. 18, no. 1, pp. 25-29, 1999, doi: 10.1053/ejvs.1999.0843.
- [10] I. Turkoglu, A. Arslan, and E. Ilkay, "An expert system for diagnosis of the heart valve diseases," *Expert Systems with Applications*, vol. 23, no. 3, pp. 229-236, 2002, doi:10.1016/S0957-4174(02)00042-8.
- [11] S. Leng, R.S. Tan, and K.T.C. Chai, C. Wang, D. Ghista and L. Zhong, "The electronic stethoscope," *BioMedical Engineering OnLine*, vol. 14, no. 66, pp. 1-37, 2015, doi: 10.1186/s12938-015-0056-y.
- [12] A. V. Muller, J. M. Amigo, N. R. Wichmann, F. B. Witschas, and F. J. Mcevor, "Fingerprinting of Doppler audio signals from the common carotid artery," *Scientific Reports*, vol. 10, no. 2414, 2020, doi:10.1038/s41598-020-59274-y.
- [13] M. Altuve, L. Suarez, and J. Ardila, "Fundamental heart sound analysis using improved complete ensemble EMD with adaptive noise," *Biocybernetics and Biomedical Engineering*, vol. 40, no.1, pp. 426-439, 2020, doi:10.1016/j.bbe.2019.12.007.
- [14] M. Sarkar, I. Madabhavi, N. Niranjana and M. Dogra, "Auscultation of the respiratory system," *Annals of thoracic medicine*, vol. 10, no. 3, pp. 158-168, 2015, doi: 10.4103/1817-1737.160831.
- [15] A. Sengur, "Support vector machine ensembles for intelligent diagnosis of valvular heart disease," *Journal of Medical Systems*, vol. 36, no. 4, pp. 2649-2655, 2012, doi: 10.1007/s10916-011-9740-z.
- [16] M. Deng, T. Meng, J. Cao, S. Wang, J. Zhang, and H. Fan, "Heart sound classification based on improved MFCC features and convolutional recurrent neural networks," *Neural Networks*, vol. 130, pp. 22-32, 2020, doi:10.1016/j.neunet.2020.06.015.
- [17] S. Reichert, R. Gass, C. Brandt, E. Andres, "Analysis of respiratory sounds: state of the art," *Clinical Medicine Insights: Circulatory, Respiratory and Pulmonary Medicine*, vol. 2, pp. 45-58, 2008, doi: 10.4137/ccrpm.s530.
- [18] I. Guler and S. Kara, "Detection of mitral stenosis by a pulsed Doppler flowmeter and autoregressive spectral analysis method," *Proceedings of the First Regional Conference, IEEE Engineering in Medicine and Biology Society and 14th Conference of the Biomedical Engineering Society of India, An International Meet*, 1995, pp. 2/91-2/92, doi: 10.1109/RCEMBS.1995.532173.
- [19] I. Guler and E. D. Ubeyli, "A recurrent neural network classifier for Doppler ultrasound blood flow signals," *Pattern Recognition Letters*, vol. 27, no. 13, pp. 1560-1571, 2006, doi: 10.1016/j.patrec.2006.03.001.
- [20] S. Ozsen, S. Kara, F. Latifoglu and S. Gunes, "A new supervised classification algorithm in artificial immune systems with its application to carotid artery Doppler signals to diagnose atherosclerosis," *Computer Methods and Programs in Biomedicine*, vol. 88, no. 3, pp. 246-255, 2007, doi: 10.1016/j.cmpb.2007.09.002.
- [21] A. Tedim, P. Amorim and A. Castro, "Development of a system for the automatic detection of air embolism using a precordial Doppler," *36th Annual International Conference of the IEEE Engineering in Medicine and Biology Society*, 2014, pp. 2306-2309, doi: 10.1109/EMBC.2014.6944081.
- [22] S. Ismail, I. Siddiqi, and U. Akram, "Localization and classification of heart beats in phonocardiography signal – a comprehensive review," *EURASIP Journal on Advances in Signal Processing*, vol. 26, pp. 1-27, 2018, doi: 0.1186/s13634-018-0545-9.
- [23] S. -K. Teo, B. Yang, L. Feng and Y. Su, "Power spectrum analysis for classification of heart sound recording," *Computing in Cardiology Conference (CinC)*, 2016, pp. 1169-1172.
- [24] D. Kristomo, R. Hidayat, I. Soesanti, and A. Kusjani, "Heart Sound feature extraction and classification using autoregressive power spectral density (PSD) and statistics features," *AIP Conference Proceedings*, vol. 1755, no. 1, pp. 090007-1-090007-7, 2016, doi: 10.1063/1.4958525.
- [25] S. E. Schmidt, C. Holst-Hansen, J. Hansen, E. Toft and J. J. Struijk, "Acoustic Features for the Identification of Coronary Artery Disease," *IEEE Transactions on Biomedical Engineering*, vol. 62, no. 11, pp. 2611-2619, 2015, doi: 10.1109/TBME.2015.2432129.
- [26] Akanksha, P. Samanta, K. Mandana and G. Saha, "Identification of Coronary Artery Disease using Cross Power Spectral Density," *14th IEEE India Council International Conference (INDICON)*, 2017, pp. 1-6, doi: 10.1109/INDICON.2017.8487905.
- [27] V. Jindal, V. Agarwal and S. Kalaivani, "Respiratory Sound Analysis for Detection of Pulmonary Diseases," *IEEE Applied Signal Processing Conference (ASPCON)*, 2018, pp. 293-296, doi: 10.1109/ASPCON.2018.8748284.
- [28] F. Z. Gogus, B. Karlik, and G. Harman, "Identification of pulmonary disorders by using different spectral analysis methods," *International Journal of Computational Intelligence Systems*, vol. 9, no. 4, pp. 585-611, 2016, doi: 10.1080/18756891.2016.1204110.






- [29] T. -E. Chen *et al.*, "S1 and S2 Heart Sound Recognition Using Deep Neural Networks," *IEEE Transactions on Biomedical Engineering*, vol. 64, no. 2, pp. 372-380, Feb. 2017, doi: 10.1109/TBME.2016.2559800.
- [30] N. Jamal, N. Ibrahim, M. N. A. H. Sha'bani, and Z. Taat, "Detection of cardiac sound components: a pilot study," *Indonesian Journal of Electrical Engineering and Computer Science*, vol. 17, no. 3, pp. 1330-1337, 2020, doi: 10.11591/ijeecs.v17.i3.pp1330-1337.
- [31] S. Hadiyoso, D. R. Mardiyah, D. N. Ramadan, and A. Ibrahim, "Implementation of electronic stethoscope for online remote monitoring with mobile application," *Bulletin of Electrical Engineering and Informatics*, vol. 9, no. 4, pp. 1595-1603, 2020, doi: 10.11591/eei.v9i4.2231.
- [32] P. J. Fish, "Non-stationary broadening in pulsed Doppler spectrum measurements," *Ultrasound in Medicine & Biology*, vol. 17, no. 2, pp. 147-155, 1991, doi: 10.1016/0301-5629(91)90122-D.
- [33] P. Atkinson, "A fundamental interpretation of ultrasonic Doppler velocimeter," *Ultrasound in Medicine & Biology*, vol. 2, no. 2, pp. 107-111, 1976, doi: 10.1016/0301-5629(76)90018-1.
- [34] R. Scissons, "Characterizing triphasic, biphasic, and monophasic Doppler waveforms: Should a simple task be so difficult?," *Journal of Diagnostic Medical Sonography*, vol. 24, no. 5, pp. 269-276, 2008, doi: 10.1177/2F8756479308323128.
- [35] S. K. Ghosh and R. N. Ponnalagu, "A Novel Algorithm based on Stockwell Transform for Boundary Detection and Segmentation of Heart Sound Components from PCG signal," *IEEE 16th India Council International Conference (INDICON)*, 2019, pp. 1-4, doi: 10.1109/INDICON47234.2019.9030299.
- [36] D. W. Baker, "Pulsed ultrasonic Doppler blood-flow sensing," *IEEE Transactions on Sonics and Ultrasonics*, vol. 17, no. 3, pp. 170-184, 1970.
- [37] S. Haykin, *Adaptive Filter Theory 5th ed.*, New York: Pearson, 2014, doi: 10.1007/s10462-018-09679-z.
- [38] S. Ayesha, T. Mustafa, A. R. Sattar, and M. I. Khan, "Data mining model for higher education system," *European Journal of Scientific Research*, vol. 43, no. 1, pp. 27, 2010, doi: 10.1016/j.procs.2015.09.037.
- [39] D. J. Bora and A. K. Gupta, "Effect of different distance measures on the performance of k-means algorithm: an experimental study in Matlab," *International Journal of Computer Science and Information Technologies*, vol. 5, no. 2, pp. 2501-2506, 2014, doi: 10.48550/arXiv.1405.7471.
- [40] N. H. M. Johari, N. A. Malik, and K. A. Sidek, "Distinctive features for normal and crackles respiratory sounds using cepstral coefficients," *Bulletin of Electrical Engineering and Informatics*, vol. 8, no. 3, pp. 875-881, 2019, doi: 10.11591/eei.v8i3.1517.

BIOGRAPHIES OF AUTHORS








Daniel Santoso      was born in Surakarta, Indonesia. He received bachelor's degree in electronic engineering from Universitas Kristen Satya Wacana, Salatiga (UKSW), Indonesia in 2005, Master of Science (M.S.) degree in electronic engineering from Chung Yuan Christian University (CYCU), Taiwan in 2009. He has been pursuing doctoral degree since 2019 in Department of Electrical and Information Engineering, Engineering Faculty, Universitas Gadjah Mada (UGM), Yogyakarta, Indonesia. His research areas including biomedical informatics and embedded system application. He can be contacted at email: daniel.santoso@mail.ugm.ac.id.



Oyas Wahyunggoro      was born in Yogyakarta, Indonesia. He received the undergraduate degree (Ir.) in Electrical Engineering from Universitas Gadjah Mada (UGM), Yogyakarta, Indonesia in 1993, the master's degree (M.T.) in Electrical Engineering from UGM in 2001, and Ph.D. degree in automation and control system from Universiti Teknologi PETRONAS, Malaysia in 2011. Currently, he is an Associate Professor with the Department of Electrical and Information Engineering, Engineering Faculty, UGM. His research focuses are: BMS, applying intelligent system on automation and control system, and biomedical signal processing. He can be contacted at email: oyas@ugm.ac.id.



Prapto Nugroho      was born in Wonogiri, Indonesia. He received S.T. (equivalent to B.Eng.) degree in Electrical Engineering from Universitas Gadjah Mada (UGM), Yogyakarta, Indonesia in 2000, M. Eng. degree in Microelectronics from Chulalongkorn University, Bangkok, Thailand in 2007, and Dr. Eng. degree in Electronics from Kyushu University, Japan. In 2000-2005 he was with semiconductor packaging and testing companies, Yoshikawa Electronics Bintan and Omedata Electronics as a product and a test Engineer respectively. He is currently a part of Department of Electrical and Information Engineering, UGM as faculty member. He can be contacted at email: tatok@ugm.ac.id.